ACTIVE ACOUSTIC NOISE CONTROL IN DUCTS

Filipe Morais and J. M. Sá da Costa
Instituto Superior Técnico, Technical University of Lisbon,
Dept. of Mechanical Engineering / GCAR - IDMEC
Av. Rovisco Pais, 1049-001Lisboa, Portugal

Keywords: Active noise control, feedforward control, filtered-reference LMS, modified filtered-reference LMS, filtered-u, frequency domain filtered-reference LMS.

Abstract: In this paper existing classical and advanced techniques of active acoustic noise cancellation (ANC) in ducts are collected and compared. The laboratory plant used in experience showed a linear behaviour and so the advanced techniques were not used. Due to delay on the plant, the feedback classical techniques could not be applied. The best results were obtained with the modified filtered-reference LMS (MFX-LMS) and filtered-u techniques. A very important conclusion is that the quadratic normalisation is needed to maintain the algorithms always stable. In this paper 18dB of attenuation of white noise and 35 dB of attenuation of tonal noise were achieved. Thus, ANC can be applied in a real situation resulting in important noise attenuations.

1 INTRODUCTION

Acoustic noise is since a long time considered as pollution due to the diverse problems that it causes in the human being, both physical, as for instance deafness, and psychological. As a consequence, competent authorities tend to enforce restrictive laws on the allowed sound levels, and it is thus necessary to look for solutions leading to its fulfilment. On the other hand, acoustic noise is a cause of lack of productivity. By these reasons, there is a pressing need to solve the problem of acoustic noise.

In practice passive solutions for the cancellation of acoustic noise can be found by simple use of absorption and reflection phenomena. However, they are of little use for frequencies below 1000Hz. In these other cases acoustic noise cancellation (ANC) based on the principle of interference, should be used.

The idea of the ANC is 70 years old. One of the first references remounts to 1934 when P. Lueg patented some ideas on the subject (Elliot, 2001 and Tokhi *et al.*, 1992). Lueg addressed ANC in ducts and in the three-dimensional space. For ducts, Lueg considered a microphone that captured the acoustic noise. The signal from the microphone would pass through the controller and feed the loudspeaker as shown in fig. 1. The controller would result in acoustic waves emitted by the loudspeaker with the same amplitude of the acoustic noise but in phase opposition, so that the two waves would cancel each other (interference principle). This configuration is nowadays the most used in ANC applications in ducts.

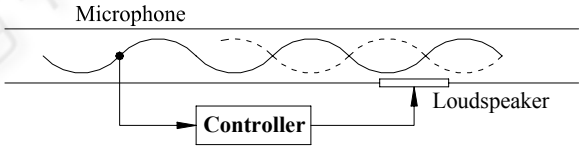

Figure 1: Single-channel feedforward control in a duct.

The purpose of using ANC in ducts is to cancel the plane waves that are propagated in the duct due to fans, like in an air conditioner installation. The ANC mostly used techniques were developed to control stochastic disturbances, because acoustic noise can be considered as a disturbance with significant spectral richness. Furthermore, techniques for stochastic disturbances can be applied in deterministic disturbances but the inverse is not feasible. ANC techniques for stochastic disturbances can be divided into two main groups: classical or advanced. Those of the first group are based on plant linearity, and consequent validity of the superposition principle (Ogata, 1997).

Linear techniques can also be applied to nonlinear systems, but they usually have bad performance. Advanced techniques were developed

Morais F. and Sá da Costa J. (2004).
ACTIVE ACOUSTIC NOISE CONTROL IN DUCTS.
In *Proceedings of the First International Conference on Informatics in Control, Automation and Robotics*, pages 214-221
DOI: 10.5220/0001141102140221

to nonlinear plants, although they can be applied to linear systems with good performance. However, they are also more complex and demand more computational power than the classic ones. For that reason advanced techniques are not preferred instead of classic ones when linear plants are concerned.

Both classic and advanced techniques can be divided according to the type of control: feedforward or feedback. In the feedforward control information is collected in advance about the disturbance and so the controller can act in anticipation; while the feedback control has no information in advance about the disturbance and thus the controller reacts to the disturbance. The feedback control is useful when the acoustic noise is created by several different sources, or by distributed sources, or when it is not practical or possible to get information in advance concerning all the noise sources. However, this is not the case of ducts because the noise source is well defined and acoustic waves are plane and travel in a single direction.

In this paper existing feedforward techniques for ANC in ducts are compared to assess the performance of these techniques in a real situation.

In ducts it is possible to have only plane acoustic waves, rending ANC much simpler since some acoustic effects are not to be found, as for instance the diffraction of acoustic waves. In this work the range of frequencies to be deal with ANC is limited to the interval [200 Hz; 1000 Hz] since ANC is not effective for frequencies above 1000 Hz and the actual set-up used does not allow to go below 200 Hz.

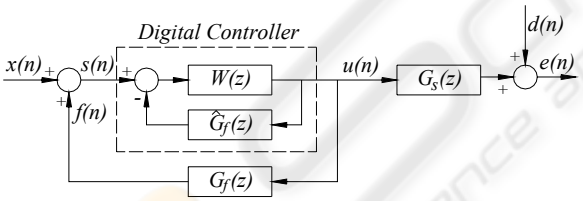

Figure 2: Block diagram of feedforward control.

2 FEEDFORWARD CONTROL

The general block diagram of the feedforward control of acoustic plane waves in a duct is found in fig. 2. The signal *x(n)* is the reference signal measured by the reference microphone, *d(n)* is the primary noise signal passed through the primary path, *e(n)* is the error signal given by the error microphone, and $G_s(z)$ is the secondary path between the secondary source and the error sensor. It is assumed that the controller is digitally implemented and made up by a direct filter *W(z)* and a feedback filter $\hat{G}_f(z)$. The feedback filter consists of an estimation of the natural feedback path of the system $G_f(z)$, i.e., reproduces the influence of the secondary source to the reference sensor. When $\hat{G}_f(z) = G_f(z)$, the two feedback loops cancel each other and the signal that feeds the controller is equal to *x(n)*. In this situation the control is purely feedforward. In the situation in which the estimate of $G_f(z)$ is not perfect, a residue appears from the cancellation of two loops. If $\hat{G}_f(z)$ is a good estimate of the path $G_f(z)$, the residue has a small value and will not affect the performance of the control. If the estimate of $G_f(z)$ is poor, this can influence the performance of the control, that may become unstable. In this situation it might be necessary to use feedback control techniques to improve the performance or to stabilize the control (Elliot, 2001).

Assuming that the two feedback loops cancel each other completely and that the plants are linear and time invariant (LTI), so that the filter *W(z)* and the discrete transfer function $G_s(z)$ can be interchanged, the error signal *e(n)* comes

$$e(n) = d(n) + \mathbf{w}^{\mathrm{T}}\mathbf{r}(n) = d(n) + \mathbf{r}(n)^{T}\mathbf{w}\,, \qquad (1)$$

where **w** is a vector with the coefficients of the filter and **r***(n)* the vector with the last samples of the filtered reference signal *r(n)* given by:

$$r(n) = \sum_{i=0}^{I-1} g_i x(n-i)\,, \qquad (2)$$

where the g_i are the I coefficients of the discrete transfer function $G_s(z)$, assuming that has a FIR structure.

2.1 Filtered-reference LMS (FX-LMS) Algorithm

This algorithm is based on the steepest descent algorithm, which is mostly used for adapting FIR controllers (Elliot, 2001). The expression for adapting the coefficients of controller *W(z)* of fig. 2 is given by:

$$\mathbf{w}(n+1) = \mathbf{w}(n) - \mu\frac{\partial J}{\partial \mathbf{w}} \qquad (3)$$

where J is a quadratic index of performance, equal to the error signal squared $e^2(n)$, and $\partial\cdot/\partial\mathbf{w}$ is the gradient:

$$\frac{\partial J}{\partial \mathbf{w}} = 2E\left[\mathbf{r}(n)e(n)\right] \qquad (4)$$

For this algorithm a simpler version than the one given by eq. (4) is used, since the expected value of the product is not reckoned, but only the current value of the gradient. Thus,

$$\frac{\partial e^2(n)}{\partial \mathbf{w}} = 2e(n)\frac{\partial e(n)}{\partial \mathbf{w}} = 2e(n)\mathbf{r}(n) \quad (5)$$

The expression for adapting the coefficients of the controller is given by:

$$\mathbf{w}(n+1) = \mathbf{w}(n) - \alpha\hat{\mathbf{r}}(n)e(n) \quad (6)$$

where $\alpha = 2\mu$ is the convergence coefficient and $\hat{r}(n)$ is the estimate of the filtered reference signal, obtained with the estimate of the $G_s(z)$ model. The algorithm is called filtered-reference LMS because the filtered reference signal is used to adapt the coefficients. The block diagram of the algorithm is in given in fig. 3.

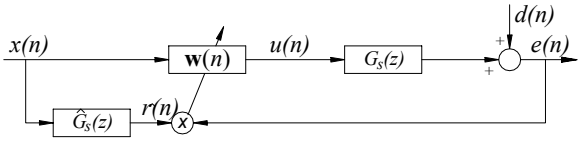

Figure 3: Block diagram for FX-LMS algorithm.

If the reference signal *x(n)* were used instead of the filtered reference *r(n)* to adapt the coefficients, the adaptation would be wrong because there is a time shift between the signal *x(n)* and the error signal *e(n)*. This is a consequence of the existence of a time delay in $G_s(z)$. This algorithm is rather simple to implement and is numerically stable, being therefore frequently used (Elliot, 2001).

2.2 Normalized filtered-reference LMS algorithm (NFX-LMS)

In the previous approach the adaptation of the coefficients of the controller *W(z)* is directly proportional to the coefficient of convergence α and the vector **r***(n)*. Sometimes, when **r***(n)* has large values, the FX-LMS algorithm has a problem of amplification of the gradient noise (Haykin, 2002). The coefficients of the vector **r***(n)* are normalized in order to solve this problem. Haykin (2002) suggests dividing the coefficients by the Euclidean norm of vector **r***(n)*. The expression for adapting the coefficients becomes:

$$\mathbf{w}(n+1) = \mathbf{w}(n) - \frac{\tilde{\alpha}}{\delta + \|\mathbf{r}(n)\|^2}\mathbf{r}(n)e(n) \quad (7)$$

where δ it is a very small and positive number. This term allows preventing numerical difficulties when **r***(n)* is small because the Euclidean norm takes small values. Elliot (2001) suggests another solution where the coefficients of vector **r***(n)* are divided by the inner product of vector **r***(n)*, $\mathbf{r}^T\mathbf{r}$. Whatever the option is, algorithm NFX-LMS presents the following advantages over algorithm FX-LMS: faster convergence rate and sometimes better performance of the obtained controller; the algorithm is more stable when there is a change of the spectral richness of the reference signal *x(n)*. This normalization of the filtered reference signal can be applied to other algorithms.

2.3 Leaky LMS algorithm

For this algorithm another index of quadratic performance is used:

$$J_2 = E\left[e^2(n)\right] + \beta\mathbf{w}^T\mathbf{w} \quad (8)$$

where β is a positive constant. This performance index weighs both the average of the error signal *e(n)* squared as well as the sum of the squares of the coefficients of the controller. This performance index prevents the coefficients of the controller from taking large values that can render the algorithm unstable when both the amplitude of the reference signal, *x(n)*, and its spectral components undergo variations (Elliot, 2001). The adaptation becomes:

$$\mathbf{w}(n+1) = (1-\alpha\beta)\mathbf{w}(n) - \alpha\hat{\mathbf{r}}(n)e(n)\,. \quad (9)$$

Eq. (9) is different for the FX-LMS algorithm because of term (1-$\alpha\beta$), which is called leakage factor. This term must take values between 0 and 1 and is normally 1. When it takes another value the error signal *e(n)* is not zero and the value of coefficients decreases with each iteration. Adding the term (1- $\alpha\beta$) to the coefficients adapting equation allows the increasing of the robustness of the algorithm. On the other hand the term (1- $\alpha\beta$) reduces the noise attenuation that can be reached. Thus, the choice of the value for beta must take into account the robustness of the algorithm and the reduction of the attenuation. In most applications, the use of a small value of beta allows a sufficient increase of robustness and the attenuation of the acoustic noise suffers little (Elliot, 2001). The modification introduced in the FX-LMS algorithm can also be implemented in the other algorithms.

2.4 Modified filtered-reference LMS algorithm (MFX-LMS)

The FX-LMS algorithm requires a rather slow adaptation compared with the plant dynamics so that the error may be given by eq. (1). This is because adapting the coefficients is somehow a nonlinearity which influence depends on the speed of adaptation (Elliot, 2001). Thus, to make this influence negligible the adaptation of the coefficients must be very slow when compared with the dynamics of the plant. This

should be regarded as a disadvantage. The arrangement shown in fig. 4 allows overcoming this limitation. In this scheme, the estimated filtered reference signal, $\hat{r}(n)$, in the adaptation path of the controller is common to the adaptive filter and to the adaptation, and has no time shift in relation to the modified error, $e'_m(n)$.

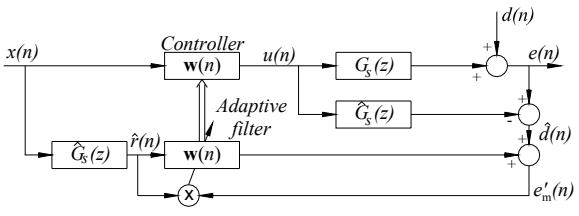

Figure 4: Block diagram for MFX-LMS algorithm.

For this algorithm the adaptation is given by:

$$\mathbf{w}(n+1) = \mathbf{w}(n) - \alpha \hat{\mathbf{r}}(n) e_m(n) \tag{10}$$

where $e_m(n)$ is the modified error, given by:

$$e_m(n) = \hat{d}(n) + \sum_{i=0}^{I-1} \sum_{j=0}^{J-1} w_i(n) \hat{g}_j x(n-i-j) \cdot \tag{11}$$

The modified error can be seen as a prediction of the error for the case where the coefficients of the controller do not change at each instant. The MFX-LMS algorithm usually presents convergence rates larger than those of the FX-LMS algorithm (Elliot, 2001). This is because the adaptive filter and the plant estimate were interchanged and thus the delay between the exit of the controller and the error signal was eliminated. For this reason it is no longer necessary to consider the delay in the restriction of the convergence coefficient, and larger steps may be used with the MFX-LMS algorithm. However the MFX-LMS algorithm has the disadvantage of requiring more computational means.

2.5 Frequency domain filtered-reference LMS algorithm (FX-LMS Freq)

For the FX-LMS algorithm the estimate of the gradient of eq. (5) was used to adapt the coefficients of the controller. The estimate of the gradient will be assumed to be given by the average of the product $\mathbf{r}(n)e(n)$ during N instants. Thus, the adaptation is given by:

$$\mathbf{w}(n+N) = \mathbf{w}(n) + \frac{\alpha}{N} \sum_{l=n}^{n+N-1} \mathbf{r}(l) e(l) \tag{12}$$

In this case, the adaptation is carried only after N time samples. The use of the average of the product $\mathbf{r}(n)e(n)$ during N instants can be considered as a more precise estimate of the gradient than the use of the product $\mathbf{r}(n)e(n)$ for each time sample. In practice adaptation with eq. (12) has a convergence rate very similar to the FX-LMS algorithm, since though the adaptation for eq. (12) has a lower frequency, the value of the update of the coefficients is larger (Elliot, 2001). The summation in eq. (12) can be thought of as an estimate of the crossed correlation between the filtered reference $r(n)$ and the error signal $e(n)$. The estimate must be reckoned from $i = 0$ up to $I-1$, where I is the number of coefficients of the adaptive filter. For long filters the reckoning of the estimate can be inefficient in the time domain, requiring a large computational effort. For large values of I it is more efficient to calculate the cross correlation in the frequency domain. If discrete Fourier transform (DFT) with 2N points for the signals $e(n)$ and $r(n)$ are considered, an estimate of the cross spectral density can be calculated through:

$$\hat{S}_{re}(k) = R^*(k) E(k) \tag{13}$$

where k is the index of discrete frequency and * means the complex conjugate. Some care must be taken to prevent the effect of circular convolution. Thus, before reckoning the DFT of the error signal, $e(n)$, with 2N points, in the block with 2N points of the error signal the first N points must be zero. This will eliminate the non-causal part of the cross correlation (Elliot, 2001). The expression that gives the adaptation of the coefficients is:

$$\mathbf{w}(m+1) = \mathbf{w}(m) - \alpha IFFT\left\{ R_m^*(k) E_m(k) \right\}_+ \tag{14}$$

where $\{\ \}_+$ means the causal part of the cross correlation, IFFT is the inverse fast Fourier transform and α is the convergence coefficient. $R_m(k)$ is directly obtained multiplying the DFT of the reference signal $X(k)$ by the frequency response estimate of the system. This algorithm is called fast LMS. Fig. 5 shows the block diagram of this algorithm.

The advantage of the fast LMS algorithm over the FX-LMS is that it requires few computations. Assuming that the implementation of the DFT requires $2N \log_2 2N$ multiplications, the FX-LMS algorithm requires $2N^2$ calculations per iteration while fast LMS needs $(16 + 6 \log_2 2N) N$.

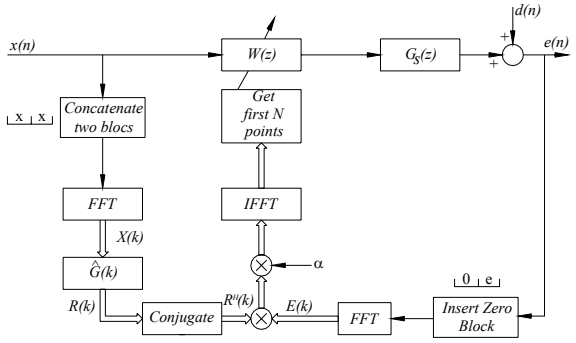

Figure 5: Block diagram for FX-LMS Freq algorithm.

2.6 Filtered-u Algorithm

Up to now Finite Impulse Response (FIR) filters have been considered to build the controllers. However, Infinite Impulse Response (IIR) filters can be used as well. In this case, the equivalent to fig.2 for IIR controllers is shown in fig. 6.

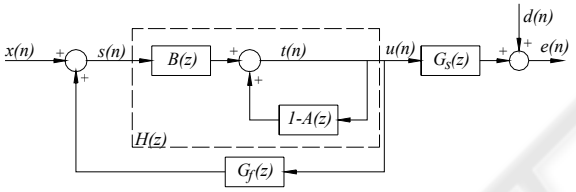

Figure 6: Block diagram for IIR controller.

Compared with the block diagram of fig. 2 for the FIR controllers, we can notice that this does not possess a specific feedback to cancel the natural feedback path of the system. In this case the recursive characteristic of IIR controllers is assumed to deal with the feedback path problem. However, practice shows that if this estimation is included numerical stability is guaranteed and the performance is improved.

The filtered-u algorithm uses IIR filter as controller. It is based on the recursive LMS (RLMS) algorithm (see Elliot (2001) or Haykin (2002)). Fig. 7 shows the block diagram of the filtered-u algorithm. The adaptation of the coefficients a_j and b_i is given by:

$$\mathbf{a}(n+1) = \gamma_1 \mathbf{a}(n) - \alpha_1 e(n)\mathbf{t}(n) \quad (15)$$

$$\mathbf{b}(n+1) = \gamma_2 \mathbf{b}(n) - \alpha_2 e(n)\mathbf{r}(n) \quad (16)$$

where α_1, α_2 are the convergence coefficients, *t(n)* and *r(n)* are respectively the filtered output and the filtered reference, and γ_1 and γ_2 are the forgetting factors.

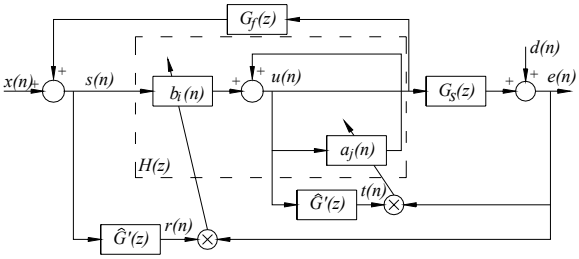

Figure 7: Block diagram for filtered-u algorithm.

The use of different convergence coefficients may be shown in practice to allow for higher convergence rates and the use of leakage factors slightly under 1 allows for a greater robustness of the algorithm (Elliot, 2001). The plants modified response, *G'(z)*, is equal to $G_s(z)$. For that purpose, the coefficients of the controller *H(z)* are assumed to be very slowly adapted in comparison to the dynamics of the system of the system $G_s(z)$. The same had already been assumed for the adaptation of the FIR controller, but for the adaptation of the IIR controller this is even more necessary since the controller is recursive. One of the interesting characteristics of the filtered-u algorithm is that it presents a self-stabilising behaviour that is also to be found in RLMS algorithms (Elliot, 2001). During the adaptation of the controller, if a pole leaves the unit-radius circle, the natural evolution of filtered-u algorithm brings it back inside. Although some researchers have addressed this behaviour, still it was not possible to discover the mechanism that results in this self-stabilising property (Elliot, 2001). The self-stabilising behaviour is found in many practical applications, and that is why the filtered-u algorithm is the most used in active cancellation of noise applications (Elliot, 2001).

3 EXPERIMENTAL SET-UP

The experimental set-up used is shown in Fig. 8. A PVC pipe with 0.125 m of diameter and 3 m of length was used for simulating the cylindrical duct. Given the diameter of the duct, the cut-on frequency, which is the frequency above which waves may no longer be considered plane, is 1360 Hz. To simulate the acoustic noise to cancel a conventional loudspeaker was placed in one of the ends of the duct. At 1.25 m away from this end two loudspeakers are placed to act as source of acoustics waves for noise cancellation. For the detection of acoustic noise a microphone, placed 0.08 m away from the primary noise source, is used. The error microphone is placed at the opposite end of the primary noise source.

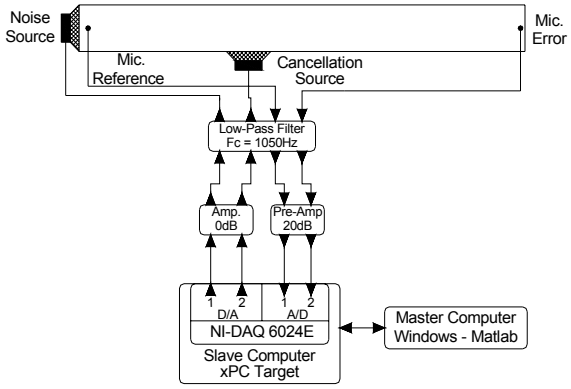

Figure 8: Block diagram of experimental setup.

Besides the duct, loudspeakers and microphones, the experimental set-up consists of: four low-pass filters that allow filtering the signals to remove the effects of aliasing and zero-order-hold; an amplifier that allows amplifying the signals that feed the loudspeakers; pre-amplifiers for the microphones; and two computers, one the slave act has a digital controller and the other the master is used for data analysis. The slave computer is a Pentium III 733MHz with 512MB of RAM memory, running on xPC Target, having a data acquisition board NI-DAQ 6024E. Algorithms have been implemented as S-Functions in the Matlab/Simulink environment.

Due to hardware restrictions on the cancellation source this set-up cannot generate relevant signals for frequencies below 200 Hz. Therefore, the frequency range where acoustic noise cancellation is intended is restricted to the frequency bandwidth of [200 Hz - 1000 Hz].

4 IDENTIFICATION

The models used are discrete in time since the implementation of the controller is made using a digital computer. Therefore, the simulations will be based on discrete models. This requires the models to include the devices associated with the discretisation and restoration of the signals, A/D and D/A conversions, anti-aliasing and reconstruction filters, and the dynamic of the microphones, loudspeakers and amplifiers associated to the experimental set-up. Assuming that the behaviour of these devices is linear, then each one can be represented by a discrete transference function. The necessary models are:

$G_s(z)$ - secondary acoustic path: includes computer - secondary source - error microphone - computer;
$G_f(z)$ - acoustic feedback path: includes computer-secondary source - reference microphone-computer.

Models have been obtained for the sampling frequency of 2500 Hz (sampling time 0.4ms) because that allows the Nyquist frequency of 1250Hz, to be slightly larger than the superior limit of the frequency range to cancel, 1000 Hz. FIR and ARX models have been obtained. Variance account for (VAF) criterion and root mean square (RMS) have been used for models validation. Table 1 shows the results obtained in these identifications.

Table 1: Order, VAF and RMS of the obtained models.

Model	*Order*			*VAF (%)*		*RMS (V)*	
	FIR	*ARX*					
	I	n_a	n_b	*FIR*	*ARX*	*FIR*	*ARX*
$G_s(z)$	500	150	150	99.96	99.94	0.0193	0.0195
$G_F(z)$	450	150	150	99.60	99.57	0.0363	0.0373

As shown above the obtained models have excellent performances. This shows the plant to have a linear behaviour being unnecessary to appeal to ANC advanced techniques.

5 EXPERIMENTAL RESULTS

The previously mentioned algorithms have been implemented and test for different noise conditions in the duct. However, before presenting the results it must be point out that the use of the normalisation of the filtered reference signal was very important. Experiences have shown that the normalised LMS technique has a significant influence in the behaviour of the algorithms. In fig. 9 the evolution of the attenuation is shown for the FX-LMS algorithm when the variance of white noise changed, for the following cases: the filtered reference signal was not normalized, was normalised using the Euclidean norm, and was normalised using quadratic normalization. The behaviour of the other algorithms is similar. In the figures that follow, attenuation is given by the expression

$$Attenuation\ (dB) = 10\log_{10}\left(\frac{E\left[e^2\right]}{E\left[d^2\right]}\right) \qquad (18)$$

where e is the error signal, d the disturbance and $E[\ ]$ is the expected value operator. In this case the expected value is given by the average of last 50 samples.

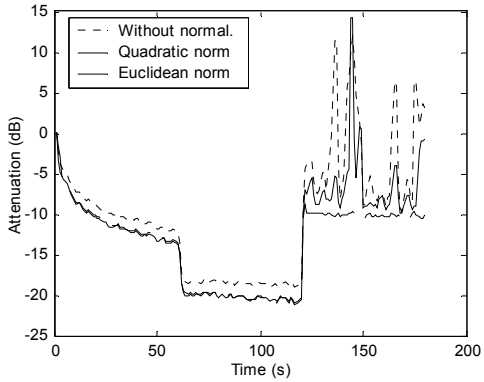

Figure 9: Evolution of attenuation for the FX-LMS algorithm.

As can be observed the normalization of the filtered reference signal allows obtaining higher attenuations. The quadratic norm is the only one that ensures the stability of the algorithms when the spectral power changes. If this were not the case different adaptation steps would have to be used to keep the algorithms stable.

For the comparison of the algorithms two types of disturbances had been considered: white noise and pure tones. The frequency range of the white noise is [200 Hz; 1000 Hz], for the reason explained before. Tones under 200 Hz have also not been used. Parameters in the algorithms were chosen based upon other experiences that had shown the influence of parameters in algorithms performance. These values are:

- FX-LMS: $w = 200$, $\mu = 0.10$;
- MFX-LMS: $w = 400$, $\mu = 0.1$;
- Filtered-u: $n_a = 150$, $n_b = 100$, $\mu_a = 0.01$, $\mu_b = 0.025$;
- FX-LMS Freq: $w = 256$, $\mu = 0.16$.

Common to all the algorithms are the leakage factor, equal to one, and the normalization method, which was the quadratic norm.

Results are shown in fig. 10-13 for different types of noise to be cancelled, and Table 2 that indicates the computational burden for the white noise case.

- White noise

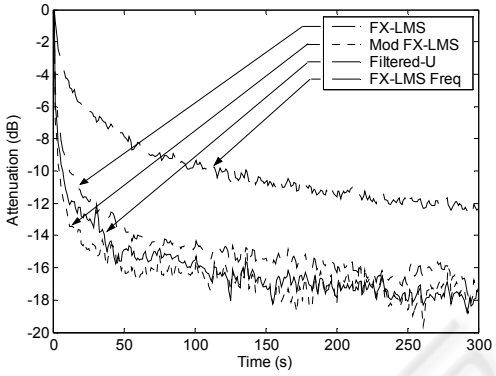

Figure 10: Evolution of attenuation for white noise.

Table 2: Execution time of each iteration for the white noise case.

Algorithm	FX-LMS	MFX-LMS	Filtered-u	FX-LMS Freq
Average time *(ms)*	0.044	0.067	0.081	0.027
Maximum time *(ms)*	0.047	0.081	0.089	0.065

- Pure tones: 320 Hz + 640 Hz + 960Hz.

All pure tones have the same spectral power. The adaptation steps of FX-LMS and FX-LMS Freq algorithms had to be reduced so that they would remain stable. Steps used were $\mu = 0{,}03$ for the FX-LMS and $\mu = 0{,}06$ for the FX-LMS Freq.

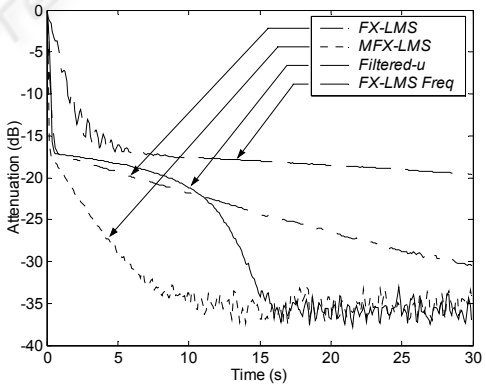

Figure 21: Evolution of attenuation for pure tones.

The two previous figures show that the MFX-LMS algorithm obtains a larger attenuation sooner but the filtered-u algorithm obtains slightly larger attenuations. These two algorithms get the best performances of the four. Worst of them all is the FX-LMS Freq, even though it presents the most reduced average time for executing each iteration. This shows how efficient algorithms are in the frequency domain. However, the execution time of each iteration is not important in this case since all times are clearly under the sampling time of 0.4ms.

This is because of the high computational power of the slave computer.

Robustness to the variations of the model of the feedback path

An important question is the robustness to the degradation of the model of the acoustic feedback path $G_f(z)$, since when this model becomes poor the simplification assumed on point 2.1 (that the model cancels the feedback path exactly) is no longer verified. If the residual of the cancellation is large, the performance of the algorithms based on scheme of Fig. 2 will degrade and may even be unstable.

The filtered-u algorithm can deal with the feedback path problem. However, using the model of Fig. 6, this algorithm has revealed to be unstable on start. To solve this problem the adaptation steps had to be reduced, and thus, have a slower evolution of attenuation. Using the scheme of fig. 2 with filtered-u algorithm has proved to be more robust and have a faster and more regular evolution of attenuation.

That is why two experiences have been carried out in which the performance of estimated model of $G_f(z)$ was reduced. In the two following figures the results for the MFX-LMS algorithms and filtered-u algorithms are shown. Only those are shown because they are the ones with better performances, as was seen above. Parameters used in the algorithms are those given above.

Figures 12 and 13 show that the filtered-u algorithm is more robust to variations of the estimated model of $G_f(z)$ model even though it leads to more irregular evolutions. This shows that the filtered-u algorithm is the one that should be applied in practice since it has a performance identical to the MFX-LMS but is more robust to modelling errors.

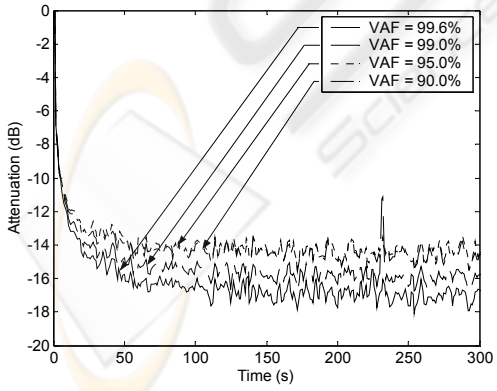

Figure 12: Evolution of attenuation for MFX-LMS algorithm for different estimated models of $G_f(z)$.

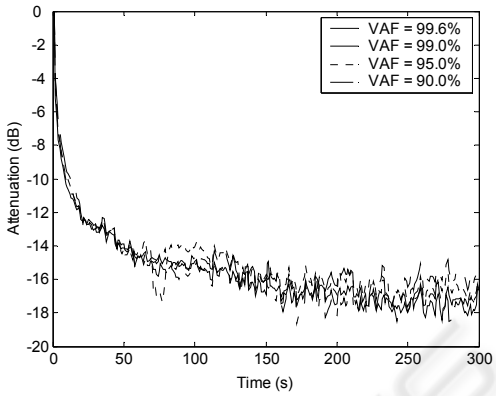

Figure 13: Evolution of attenuation for filtered-u algorithm for different estimated models of $G_f(z)$.

6 CONCLUSIONS

This paper evaluates the use of feedforward ANC to cancel noise in ducts. The *FX-LMS, NFX-LMS, Leaky LMS, MFX-LMS, FX-LMS Freq* and the *Filtered-u* algorithms have been considered. The best performance was achieved with the filtered-u algorithm. Active cancellation of acoustic noise was seen to be possible in practice since attenuations obtained were about 18 dB for white noise and 35 dB for pure tones. Moreover, algorithms were seen to be robust when models degrade.

In what concerns the algorithms it was shown that the normalization of the filtered reference signal is of extreme importance allowing to ensure the stability of the algorithms as well as better attenuations. However this happens only for the quadratic norm.

REFERENCES

Elliot, S. J., 2001. *Signal Processing for Active Control*. Academic Press, London.

Haykin, Simon, 2002. *Adaptive Filter Theory*. Prentice Hall, New Jersey, 4th edition.

Ogata, Katsuhiko, 1997. *Modern Control Engineering*. Prentice Hall, New Jersey, 3rd edition.

Oppenheim, Alan V., Schafer, Ronald W. and Buck, John R., 1999. *Discrete-time Signal Processing*. Prentice Hall, New Jersey, 2nd edition.

Tokhi, M. and Leitch, R. R., 1992. *Active Noise Control*. Oxford University Press, New York.